DOI:10.1158/1535-7163.MCT-05-0040

Molecular Cancer Therapeutics

p37 induces tumor invasiveness

Catherine M. Ketcham, Satoshi Anai, Robbie Reutzel, et al.

Mol Cancer Ther 2005;4:1031-1038. Published online July 14, 2005.

DOI:10.1158/1535-7163.MCT-05-0040

p37 induces tumor invasiveness

Catherine M. Ketcham,[1] Satoshi Anai,[3] Robbie Reutzel,[1] Shijie Sheng,[4] Sheldon M. Schuster,[1] Ryan B. Brenes,[1] Mavis Agbandje-McKenna,[1] Robert McKenna,[1] Charles J. Rosser,[3] and Susan K. Boehlein[1,2]

[1]Department of Biochemistry and Molecular Biology and [2]Shands Cancer Center, College of Medicine, University of Florida, Gainesville, Florida; [3]Division of Urology, College of Medicine, University of Florida, Jacksonville, Florida; and [4]Department of Pathology, Wayne State University School of Medicine, Detroit, Michigan

Abstract

Previous studies have shown a statistically significant correlation between human carcinomas and monoclonal antibody detection of a *Mycoplasma hyorhinis*–encoded protein known as p37. A potential mechanism of p37 is that it might promote invasion and metastasis. Recombinant p37 enhanced the invasiveness of two prostate carcinoma and two melanoma cell lines in a dose-dependent manner *in vitro*, but did not have a significant effect on tumor cell growth. Furthermore, the increased binding to cell surfaces and the enhanced invasive potential of cancer cells from exposure to p37 could be completely reversed by preincubation of the cancer cells with an anti-p37 monoclonal antibody. Sequence comparisons, followed by three-dimensional molecular modeling, revealed a region of similarity between p37 and influenza hemagglutinin A, a sialic acid–binding protein that plays a critical role in viral entry. Binding of p37 to prostate carcinoma cells was found to be at least partially sialic acid dependent because neuraminidase treatment decreased this binding. Taken together, these observations suggest that *M. hyorhinis* can infect humans and may facilitate tumor invasiveness via p37. These results further suggest that p37 may be a molecular target for cancer therapy. [Mol Cancer Ther 2005;4(7):1031–8]

Introduction

Although it is not yet generally accepted, the involvement of *Mycoplasma* infection with the progression of human cancer has significant precedence. The search for unrecognized pathogens within the human body has been rapidly expanding (1). Many diseases such as peptic ulcers, atherosclerosis, ulcerative colitis, cervical condyloma, lymphoma, Whipple's disease, and Kaposi's sarcoma have been associated with microbial pathogens (2). Infectious agents (viruses, bacteria, and multicellular parasites) are being reexamined as contributors to human carcinogenesis, either as transforming agents themselves or by induction of a state of persistent inflammation (2). For example, the association between the common human bacterial pathogen *Helicobacter pylori* (which infects an estimated 40–80% of individuals) and development of gastric cancer has clearly shown that tumorigenesis can be initiated by chronic persistent infection with a prokaryotic agent of low virulence (3).

Mycoplasmas (class *Mollicutes*) are pleomorphic, wall-free, prokaryotic organisms that can reside either on the eukaryotic cell membranes or inside the cell. They are the smallest organisms (at 0.2–0.3 μm) capable of self-replication (4), with genomes of ~500 to 800 kbp (compared with *Escherichia coli*, which has a genome of 4,600 kbp). To date, at least 16 mycoplasmal species have been isolated from humans (5).

The importance of human-associated mycoplasmas first became apparent in the 1960s on the characterization of the novel human respiratory pathogen *Mycoplasma pneumoniae* (6–8). Since then, other mycoplasmas such as *Mycoplasma hominis* and *Ureaplasma urealyticum* have been well documented as human urogenital tract pathogens (6, 7). However, an untold number of mycoplasma infections may go unidentified because many people seem to be chronically colonized by mycoplasmas without apparent illness (9).

A number of studies of leukemia patients in the mid-1960s raised the possibility of an association between mycoplasmas and leukemia (10), and there is recent evidence linking mycoplasma infection to other types of cancer. One report indicated that 48% of tumors from patients with gastric cancer were positive for mycoplasma (11). Another study involving patients with ovarian cancer revealed a mycoplasma infection rate of 59.3% (12), and the same authors detected a relationship between cervical cancer and mycoplasma infection with 72 archived paraffin-embedded sections (13). In contrast, another group found only a 13% infection rate in ovarian cancer in 46 frozen tumor samples and concluded that there was no significant relationship between mycoplasma infection and ovarian cancer (14).

In attempts to define tumor-specific cell surface markers, several groups have either detected p37 from *Mycoplasma hyorhinis* in cancer patients or described its correlation with invasiveness in model systems. This protein was first described in an effort to identify human cell antigens that elicit tumor-specific antibodies. Fareed et al. (15) analyzed the immune response in a group of cancer patients who were immunized intralymphatically with tumor cell extracts. Sera from patients who were in a state of tumor regression

Received 2/8/05; revised 4/12/05; accepted 4/29/05.

Grant support: University of Florida Research Opportunity Fund (S.M. Schuster), University of Florida Alumni Fellowship (R. Reutzel), University of Florida, College of Medicine start-up funds (R. McKenna), NIH grant CA84176 (S. Sheng), and the Ruth Sager Memorial Fund (S. Sheng).

Note: S.M. Schuster is currently at Keck Graduate Institute, Claremont, CA 91711.

Requests for reprints: Susan K. Boehlein, Department of Biochemistry and Molecular Biology, College of Medicine, University of Florida, Gainesville, FL 32610. Phone: 352-392-0032; Fax: 928-962-0569. E-mail: sboehlei@ufl.edu

DOI:10.1158/1535-7163.MCT-05-0040

showed measurable antibody titers against several antigens, including a 38 kDa protein. These antigens were not detected in those whose tumors failed to regress. The 38 kDa protein antigen was designated p37 (16), but was also called p38 kDa protein antigen (17) and p40 (18) in other reports.

When the *p37* gene was isolated and sequenced, it was shown to be of *M. hyorhinis* origin (19). The *p37* gene encodes a peptide of 403 amino acids with a molecular mass of 43.5 kDa. An analysis of the protein sequence revealed that p37 has about a 34% to 42% similarity to a periplasmic binding protein–dependent transport system found in Gram-negative bacteria and several species of mycoplasma (16, 19). Thus, p37 is thought to be part of a high-affinity transport system from *M. hyorhinis*.

Although *M. hyorhinis* has not been previously described as a human pathogen, it commonly infects swine and can be found in up to 40% of weanling pigs (20). It causes respiratory tract infections, inflammation of the lining of the chest and abdominal cavity, and arthritis (21). Nevertheless, there is preliminary evidence that strongly indicates that *M. hyorhinis* infection in humans has clinical significance.

Other studies aimed at identification of novel tumor markers also fortuitously identified p37 as a cancer-related neoantigen. Lysate from cells infected with *M. hyorhinis* was able to stimulate leukocyte adhesion inhibition responses with leukocytes from cancer patients but not from normal controls (18). Additionally, two independent research groups showed that p37 on the surface of FS9 mouse fibrosarcoma cells was associated with a highly invasive phenotype, as measured in an *in vitro* cellular invasion assay (22, 23). Furthermore, antibodies against p37 inhibited the invasive potential of infected FS9 cells in the *in vitro* assay (22, 23), and reduced the lung metastasis of colon cancer in nude mouse models (24).

It was not until recently when Huang and others showed mycoplasmal infection in a variety of 600 paraffin-embedded carcinoma tissues. A specific monoclonal antibody that recognizes the unique *M. hyorhinis*–specific protein p37 was used to detect mycoplasma infection in these samples (25). The results indicated a statistically significant correlation between the presence of *M. hyorhinis* and gastric carcinoma and colon cancer. Specifically, 56% of gastric carcinoma and 55% of colon carcinoma biopsies were positive for *M. hyorhinis*, but in other gastric diseases, such as chronic superficial gastritis, gastric ulcers, and intestinal metaplasia, the mycoplasma infection rate was significantly less.

A high-density tissue microarray containing 105 gastric cancer biopsies, 101 benign margin tissues, and 62 noncancerous tissue specimens from patients with gastric disease was then screened with the anti-p37 monoclonal antibody. It was determined that the infection rate of *M. hyorhinis* was 54.1% in gastric cancer, 51.7% in benign margin tissue, and 15.8% in noncancerous disease samples. The difference of infection rates between gastric cancer and noncancerous gastric disease was statistically significant ($P = 0.001$; ref. 26).

With the demonstration of p37 in human tumors, we felt this required further exploration. Herein we set out to show that p37 has the ability to increase the invasive behavior of cancer cells in a dose-dependent manner without affecting cell growth; the invasive potential of p37 can be blocked by antibodies raised against p37; and p37 binds in part through interaction with sialic acid. These observations suggest that p37 could potentially play a role in tumor invasion.

Materials and Methods

Cell Culture and Other Reagents

Human prostate cancer cell lines PC-3 and DU-145 were from American Type Cell Culture (Manassas, VA) and human melanoma cell lines C8161 and A375M were kind gifts from Dr. I.J. Fidler (M.D. Anderson Cancer Center, University of Texas, Houston, TX). For maintenance, PC-3 and DU-145 cells were cultured in RPMI media supplemented with 5% FCS, whereas C8161 and A375M cells were cultured in DMEM supplemented with 10% FCS. All culture media components were purchased from Invitrogen (Carlsbad, CA). Monoclonal antibody 1F6 against p37 was raised against purified recombinant p37. This antibody was made at the University of Florida ICBR hybridoma Core Facility. The secondary antibody and detection reagents for immunofluorescent staining were purchased from Zymed (San Francisco, CA). The membrane invasion culture system was purchased from the Hendrix Laboratory (University of Iowa, Iowa City, IA). Polycarbonate membrane of 8 mm pore size was purchased from Poretics (Livermore, CA). Growth factor reduced Matrigel was purchased from Becton Dickinson (Franklin Lakes, NJ). The sensitive immunofluorescent staining method of Gignac et al. (27) was routinely used to ensure that all mammalian cell cultures were free of mycoplasma contamination. Econo-Pac high S column (strong cation exchange resin), macro-prep Q column (strong anion exchange resin), and Econo-Pac S cartridge (strong cation exchanger) were obtained from Bio-Rad (Hercules, CA). Neuraminidases from *Arthrobacter ureafaciens* and *Macrobdella decora* were from Calbiochem (San Diego, CA). All other reagents unless otherwise indicated were purchased from Sigma (St. Louis, MO).

Expression and Purification of p37

Plasmid pMH38-113 contained the entire coding sequence for p37 whereby all of the TGA codons (mycoplasmal codon for Trp) were changed to TGG to optimize its expression in *E. coli*. PCR primers used to amplify the p37 coding region minus the leader sequence were 5′-ATGTGTTCTAACACCGGTGTAGTTAAG-3′ and 5′-GAATTCTTATTTAATGGCTTTTTCATAAAC-3′. The resulting cDNA fragment was 1,140 bp long. The sequence of the PCR product was confirmed identical to the published sequence (24) by DNA sequencing (DNA Sequencing Core Laboratory at the University of Florida). This product was ligated into the expression vector pET31f1m1 (gift of Dr. P. Laipis, Department of Biochemistry, University of Florida, Gainesville, FL). The resulting p37-expressing plasmid was designated as pETp37. Bacterial strain BL21 (DE3) pLysS was subsequently transformed with pETp37.

To express p37, a freshly transformed bacterial colony was used to inoculate 1 L of minimal media (37°C) supplemented

DOI:10.1158/1535-7163.MCT-05-0040

with tryptone (10 g/L), ampicillin (100 μg/mL), chloramphenicol (30 μg/mL), and glucose (0.75% w/v). When the culture reached an absorbance of 0.7 to 1.0 at 600 nm, isopropyl-L-thio-B-D-galactopyranoside was added to a final concentration of 1 mmol/L. Cells were grown for an additional 2.5 hours at 37°C and harvested.

To purify p37 from the soluble cellular extract, cells were lysed by vortexing the pellet in 1/10 the original volume of 20 mmol/L phosphate buffer (pH 7.8) followed by a sonication for three 15-second cycles. The resulting crude cell lysate was centrifuged at 40,000 × *g* for 20 minutes at 4°C to remove cell debris. The clear supernatant (soluble cellular extract) was subjected to ion exchange chromatography using the Econo System (Bio-Rad). Briefly, a 5 mL Bio-Rad Econo-Pac S cation exchange column was attached to the bottom of a 50 mL Bio-Rad anion exchange Q column, and equilibrated with 20 mmol/L sodium phosphate buffer (pH 7.95) at a flow rate of 2.5 mL/min. Approximately 125 mg of soluble cellular extract were loaded on the column. The flow-through containing p37 was adjusted to pH 6.1 with 2 mol/L acetic acid, and loaded on a 5 mL cation exchanger, Bio-Rad Econo-Pac S cartridge, equilibrated with 20 mmol/L sodium acetate, pH 6.1 (buffer A). The column was washed with 5% buffer B [20 mmol/L sodium acetate (pH 6.1), 1 mol/L NaCl] and the p37 protein was eluted with 15% buffer B. The eluted sample was then concentrated using a Centriprep 10 spin column (Millipore, Bedford MA). The yield of p37 was estimated to be ~30 mg of purified p37 from 1 L of *E. coli* or 10% w/w.

Two-Antibody Sandwich ELISA Assay for Detection of p37

Purified anti-p37 monoclonal antibody was bound to a solid support and the plate and additional binding sites were blocked with bovine serum albumin. Cell lysate (or p37 diluted in TBS-bovine serum albumin for a standard curve) was then added to the plate. A second biotinylated monoclonal antibody that does not compete with the coating antibody for binding to p37 was then added. Streptavidin conjugated to alkaline phosphatase was added, followed by the phosphatase substrate *p*-nitrophenylphosphate. These samples were then assayed in triplicate. A standard curve was prepared in duplicate ranging from 30 pg to 4 ng. The absorbance at 405 nm was directly proportional to the amount of p37 present. The GraphPad Prism program was used to analyze results and error was calculated as SD.

Cell Growth

Cells were harvested at the exponential growth phase, counted using a Z1 Coulter Counter, and seeded at 4×10^3/well in duplicate 96-well microplates in 0.2 mL maintenance media containing various concentrations of purified p37 or same concentrations of bovine serum albumin. On each indicated subsequent day, cells in one plate were quantified by the sulforhodamine B staining method (28) whereas the culture media in the remaining plates was replenished with fresh media containing p37 or bacterial extract protein. The absorbance of sulforhodamine B was measured at 550 nm using a Benchmark microplate reader (Bio-Rad).

Immunofluorescent Staining of p37

Cells were cultured in eight-well chamber slides in maintenance media until they appeared to be 80% confluent. They were then gently washed with a balanced salt solution and treated with the recombinant p37 at a final concentration of 20 μg/mL in serum-free keratinocyte growth medium for 1 hour in a humidified incubator with 6.5% CO_2. The negative control cells were incubated with serum-free keratinocyte growth medium only. The cells were gently washed thrice with PBS.

To stain cell membrane–bound antigen under non-permeabilizing conditions, the cells were fixed with freshly prepared 4% paraformaldehyde. To stain the cellular antigen under permeabilizing conditions, the cells were fixed with freshly prepared 4% paraformaldehyde plus 0.1% (v/v) Triton X-100. The cells were blocked with normal goat serum at a 1:10 dilution for 60 minutes, probed with monoclonal antibody 1F6,[5] diluted in blocking solution to a final concentration of 5 μL/mL at 0.05 mL/well), and incubated in a humidified chamber overnight at 4°C. The cells were then rinsed with three changes of PBS and probed with goat anti-mouse FITC (1:100 dilution in the blocking buffer; Zymed) for 1 hour at room temperature. The cells were washed with three changes of PBS and the cell nuclei were counterstained with 10 μg/mL Hoechst dye for 15 minutes. The cells were washed with distilled deionized water and mounted with the antifade media (Molecular Probes, Eugene, OR) and viewed under a Lica UV-fluorescent microscope (model DMIRB).

Invasion Assay

Ten-micrometer polycarbonate membranes were coated with 4 mg/mL growth factor reduced Matrigel as described (29). The cells were seeded at a density of 100,000 cells/mL/well in DFCI media (30). Proteins to be tested were added to various final concentrations as indicated. After incubation in a humidified incubator with 6.5% CO_2 at 37°C for 24 hours, the coating and the cells on the top of the polycarbonate membrane were removed. The cells attached to the bottom side of the membrane were fixed by 100% methanol, stained with LeukoStat Staining kit from Fisher, and counted using a Carl Zeiss microscope.

Neuraminidase Treatment of PC-3 Cells

The prostate tumor cell line PC-3 was grown to 85% confluency and detached from flasks by incubation in PBS containing 2 mmol/L EDTA. Cells were supplemented with metabolic inhibitors (10 mmol/L NaN_3, 5 mmol/L 2-deoxyglucose, and 2 mmol/L NaF) to deplete cellular ATP and abolish receptor-mediated endocytosis (31). Bovine serum albumin was added to all samples to a final concentration of 5 mg/mL. Terminal sialic acid residues were removed from cell-surface carbohydrates by incubation with neuraminidase from either *A. ureafaciens* (40 milliunits/mL; removes terminal α2-3,6,8-linked sialic acid residues) or *M. decora* (10 milliunits/mL; removes only terminal α2,3-linked sialic acid residues) for 4 hours.

[5] G. Fareed, personal communication.

DOI:10.1158/1535-7163.MCT-05-0040

p37 (50 μg/mL) was added after neuraminidase treatment. For the wells containing sialic acid (2.5 mmol/L) or fetuin (100 μg/mL), the compounds were mixed with p37 before addition to the cells. The viability of cells was determined by trypan blue exclusion and was >95% after 6 hours. The cells were washed and then lysed with Tissue Protein Extraction Reagent buffer (Pierce, Rockford, IL) containing protease inhibitors. The two-antibody sandwich ELISA assay was employed for the detection of bound p37.

Alignment and Model Building of p37

The p37 amino acid sequence was searched using the web-based BLAST server (32) to ascertain if there was any sequence homology with known three-dimensional protein structures in the Protein Data Base. A partial model of p37 was derived using the structure of human hemagglutinin A (A/Aichi/68), PDB accession 1HGG (33), as a template for the tertiary fold of the protein. This was achieved by interactively mutating/deleting/inserting the amino acids that differed between the known structure and the p37 sequence using the program O7 (34). The p37 model geometry was energy minimized using the software package CNS (35). Figure 4 was produced using the program BOBSCRIPT (36).

Results

p37 Binds to the Cell Surface and Stimulates Tumor Cell Invasion

Although previous correlative evidence suggests that p37 may facilitate tumor invasion, the exact mechanism by which p37 exerts an increase in tumor-invasive activity is unknown. To test this possibility, the invasive potential of prostatic cancer cell lines PC-3 and DU-145 was quantified in the presence of p37 using an established invasion assay (29). As shown in Fig. 1A, the invasiveness of prostatic cancer cells was stimulated by purified p37 in a dose-dependent manner in both PC-3 and DU-145 cells (DU-145 data not shown). Thus, p37 seems to enhance the invasive phenotype of tumor cells of different genetic backgrounds. In addition, monoclonal antibody raised against purified p37, 1F6, completely neutralized the stimulating effect of p37 (Fig. 1B). In parallel, a nonspecific antibody added at the same final concentrations did not have a significant effect on the invasiveness of either prostate cell line (Fig. 1C). Thus, the p37 effect on tumor cell invasion does not seem to require additional mycoplasma proteins. This result is consistent with the findings of Steinmann et al. (23) that Fab fragments of a monoclonal antibody directed against p37 inhibited the highly invasive phenotype of FS9 mouse sarcoma cells in culture. The above results were confirmed in melanoma cell lines C8161 and A375M (data not shown).

To clarify whether the stimulatory effect of p37 on tumor invasion was a manifestation of its effect on tumor cell proliferation, the two prostatic cancer cell lines, PC-3 and DU-145, as well as the two human melanoma cell lines, C8161 and A375M, were cultured in the presence of purified p37 or with a protein extract from *E. coli.* All cells treated with recombinant p37 exhibited similar growth kinetics as cells treated with the same amount of the total protein extract from bacteria (data not shown).

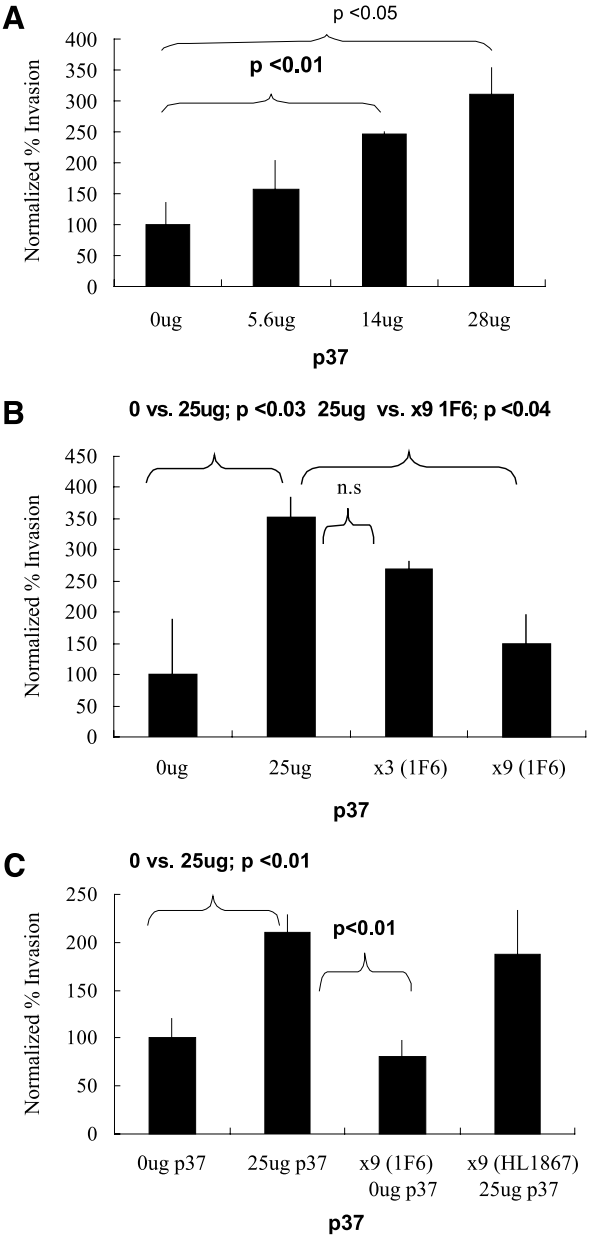

Figure 1. p37 stimulates tumor invasion *in vitro*. **A,** dose-dependent stimulatory effect of p37 on the invasive potential of the prostatic cell line PC-3 (DU-145 data not shown). **B,** dose-dependent stimulatory effect of p37 on the invasive potential of prostate carcinoma cells PC-3 treated with monoclonal antibody raised against p37 (*1F6*) blocks the invasive potential of p37. **C,** a nonspecific antibody (*HL1867*) to p37 had no effect on the action of p37. The invasion data from untreated tumor cells were normalized as 100% and invasion data from treated tumor cells were expressed as percentage of this control. *Columns,* average of triplicate results; *bars,* SE.

To test whether the p37 effect on tumor cell invasiveness is mediated by a direct interaction between p37 and the tumor cells, immunofluorescent staining of p37 was done with p37-treated prostate tumor cells. As shown in Fig. 2, a signal was not detected using a p37-specific

DOI:10.1158/1535-7163.MCT-05-0040

monoclonal antibody (2C1) in untreated cells under either nonpermeabilizing conditions (Fig. 2E and F) or permeabilizing conditions (data not shown). However, cells treated with p37 exhibited a specific immunoreactivity with a nonneutralizing p37 antibody (2C1) under both nonpermeabilizing conditions (Fig. 2A and B) and permeabilizing conditions (Fig. 2C and D). Cell membrane permeabilization did not further increase the immunoreactivity. These data suggest that p37 detected by monoclonal antibody 2C1 was primarily contributed by the cell membrane fraction.

Alignment and Model Building of p37

Having shown that p37 bound to the surface of tumor cells, it was of interest to determine if it resembled any other proteins known to bind to cell membrane components. A BLAST search revealed a partial pairwise sequence alignment of p37 (residues 186–343 and 153–254) with the distal head domain of hemagglutinin A of avian influenza virus (residues 118–271; Fig. 3A) and several β-strands of cathepsin B from *Schistosoma mansoni* (residues 228–329; Fig. 3B). Neither the three-dimensional structure of hemagglutinin A of avian influenza virus nor cathepsin B from *S. mansoni* has been determined. However, both the crystal structures for human A/Aichi/68 hemagglutinin influenza virus (37) and cathepsin B from rat (38) are known. The human fragment of the A chain of hemagglutinin (residues 123–275) has a 33% sequence identity to the avian fragment (residues 118–271), which shares a 20% sequence identity to p37 (residues 186–343). Furthermore, the rat cathepsin B (residues 138–239) has a 62% sequence identity to the *S. mansoni* form (residues 228–329), which shares a 22% sequence identity to p37 (residues 153–254). On examination of the three-dimensional structures of the two partial fragments of human hemagglutinin A and rat cathepsin B that aligned with the p37 sequence (Fig. 3), it was indicative that the COOH-terminal domain of p37 may have a propensity to form β-strands as secondary structural elements in its tertiary fold. Also, the pairwise sequence alignment of residues 186 to 343 of p37 revealed

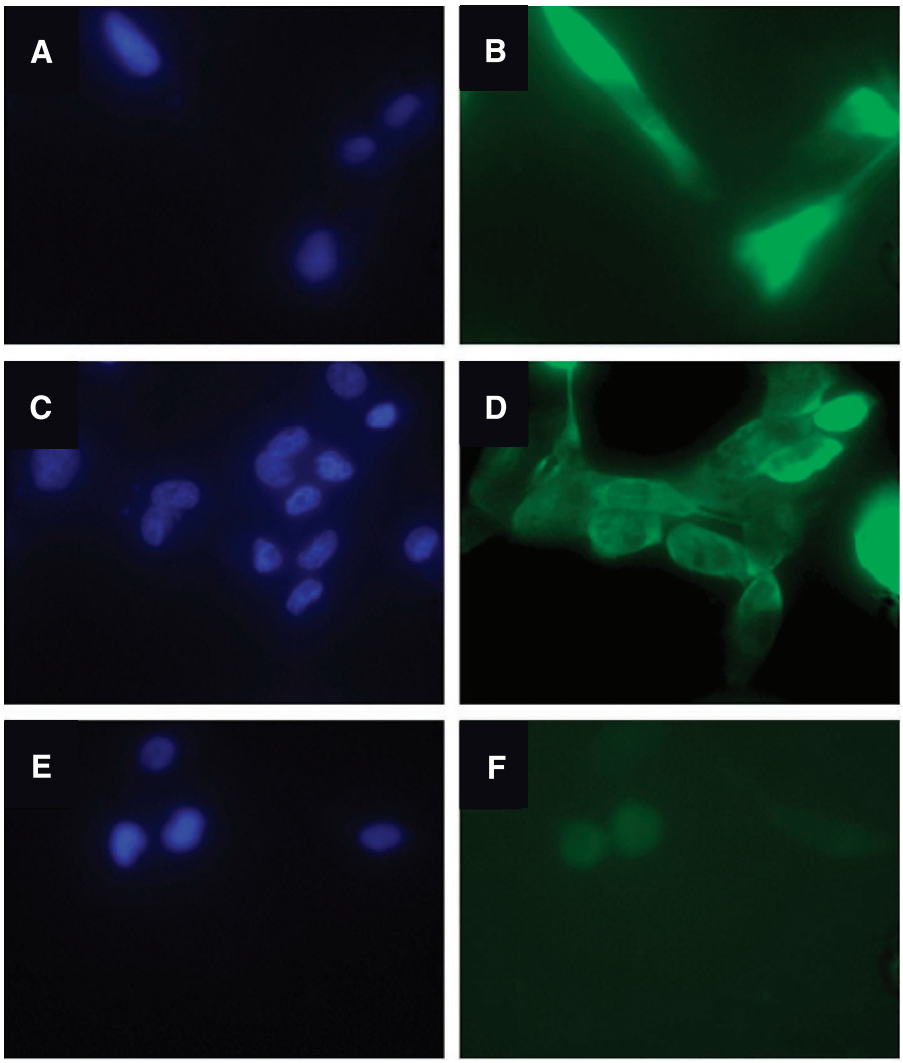

Figure 2. Immunodetection of recombinant p37 bound to PC-3 cell surface. **B, D,** and **F,** immunoreactivity of p37 (*green*). **A, C,** and **E,** staining of nuclei (*blue*) in **B, D,** and **F,** respectively. **A** to **D,** p37-treated cells; **E** and **F,** untreated cells. **A** and **B,** nonpermeabilized cells; **A** to **D,** permeabilized cells. Magnification, ×400.

DOI:10.1158/1535-7163.MCT-05-0040

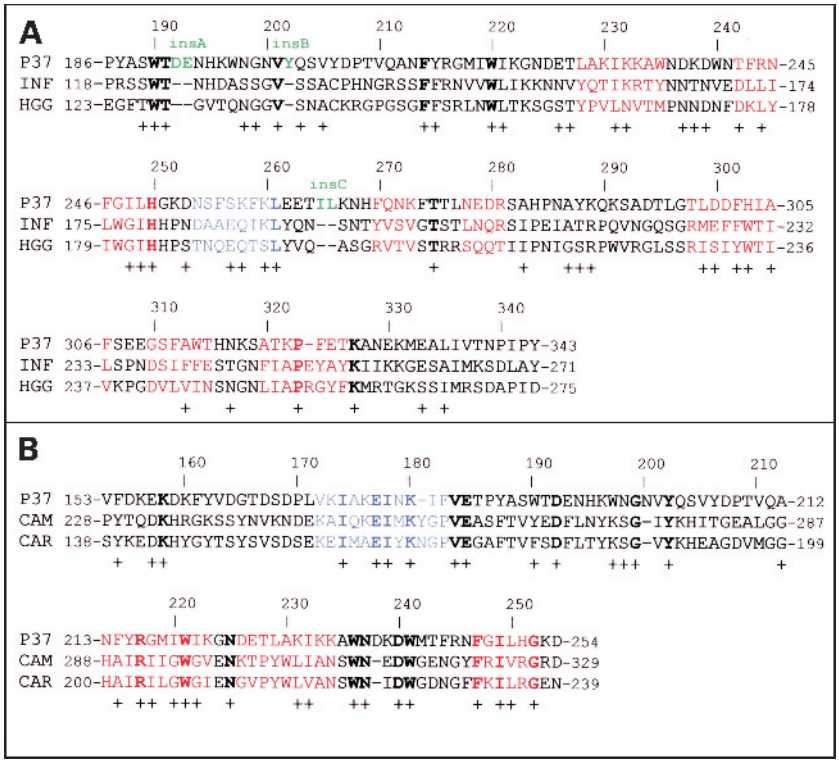

Figure 3. Sequence alignment. **A**, p37, hemagglutinin A from avian (*INF*), and human A/Aichi/68 (*HGG*) influenza virus. **B**, p37 and cathepsin B from *S. mansoni* (*CAM*) and rat (*CAR*). *Bold letters,* residues that are conserved in compared sequences; *red* and *blue,* residues that are known to form β-strands and α-helices, respectively. The sequence numbers of p37 are given on the top and similar-type residues are depicted as plus signs on the bottom of each alignment. Residue numbers of comparison sequences to p37 given at the start and end of each line.

that it most likely shares the jelly role motif (β-strands S2–8) of the distal head domain of hemagglutinin A (residues 118–271; Fig. 4A and B). Based on these observations, a model of the COOH-terminal domain of p37 (residues 186–343) was built (Fig. 4C). On examination of the model, it was remarkable that most of the conserved residues in the known sialic acid binding site of hemagglutinin were conserved in the p37 model, having a binding pocket lined with hydrophobic residues (Table 1).

To determine whether p37 binds to its target receptor through sialic acid, a whole cell ligand binding assay was developed. It was used to determine whether neuraminidase (sialidase) treatment of cells diminishes the binding of p37. Two distinct neuraminidases were used to determine whether p37 is able to distinguish between the two major sialic acid (NeuAc) linkages on cell surface carbohydrates, NeuAcα2,3Gal and NeuAcα2,6Gal. The results are shown in Table 2. Treatment of cells with neuraminidase of broad specificity decreased the binding of p37. Furthermore, binding seems to be at least partially specific for α2,3-linked sialic acid residues. Surprisingly, addition of free sialic acid, or fetuin, a glycoprotein rich in both α2,3- and α2,6-linked sialic acid, enhanced binding of p37 to the cells (Table 2).

Discussion

Although *M. hyorhinis* and p37 have long been associated with increased invasiveness and tumor metastasis (17–26), this report reveals that purified recombinant p37 bound to cell surfaces stimulated the invasiveness of human cell lines (Fig. 1). This is the first study to indicate that p37 alone is sufficient to enhance at least one pathway involved in cell invasion. These data also provide the functional evidence for a tumor-promoting role of p37 that could help explain the previous clinical finding that autoimmunity against p37 correlates with a better prognosis for melanoma, ovarian, prostate, and renal cancers (15). The evidence that p37 did not have a significant effect on the growth rate of two prostate carcinoma cell lines suggests that p37 may not be involved in the mycoplasma metabolic machinery that adds additional stress to the host cells (data not shown). On the other hand, it remains a possibility that p37 may affect the growth or survival of more differentiated or normal cells.

It has been reported that p37 is structurally similar to components of a periplasmic binding protein–dependent transport system in bacteria (16, 19). Interestingly, a further sequence comparison revealed a striking resemblance (41% similarity) of p37 to the hemagglutinin protein from influenza A (Fig. 3). Detailed structural and functional studies of hemagglutinin A (37–40) show that this molecule binds to the host cell surface receptor and plays a critical role in viral entry (41). Several of the residues conserved between hemagglutinin A and p37 are those that seem to be critical for hemagglutinin A binding to the cell surface (Table 2). The modeling of p37 reveals the COOH-terminal domain as a jelly role motif (β-strands S2–8) having a highly conserved hydrophobic pocket, similar to the distal head domain of hemagglutinin A (Figs. 3 and 4). This suggests that p37 possesses a sialic acid binding site which may have a

DOI:10.1158/1535-7163.MCT-05-0040

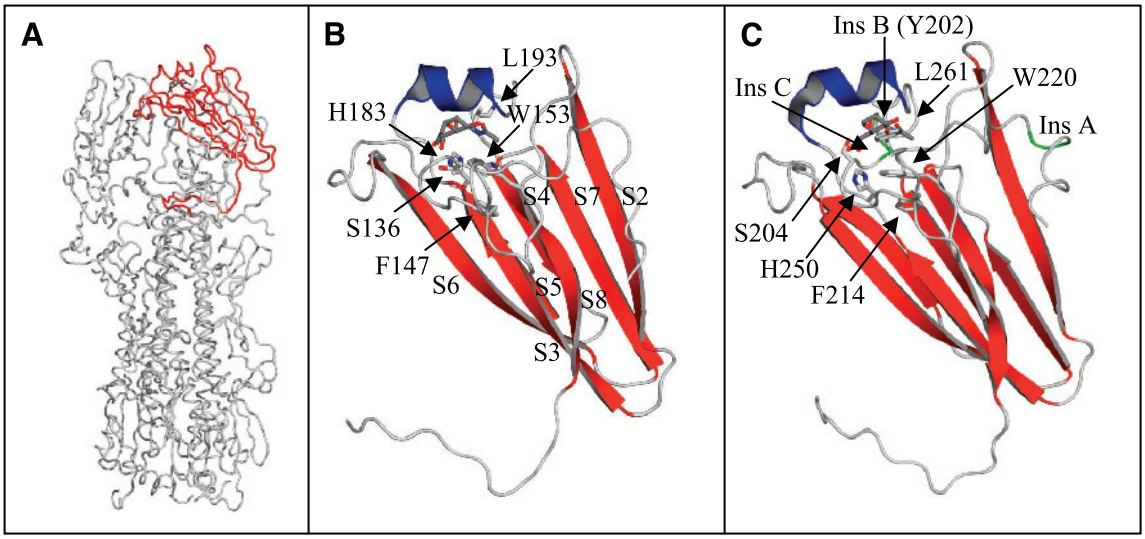

Figure 4. **A,** structure of the human hemagglutinin (A/Aichi/68) trimer, residues 123 to 275 of one of the A chains of the distal tip, which shares sequence homology with residues 186 to 343 of p37, highlighted in red. **B,** ribbon diagram showing the secondary structural elements of the red highlighted residues in **A**. Active site residues associated with sialic acid binding (Table 1) are depicted as ball and sticks. Sialic acid is depicted as a black ball and stick model. β-Strands and α-helices are colored red and blue, respectively. **C,** ribbon diagram of the p37 model based on the pairwise sequence alignment shown in Fig. 3. Conserved residues associated with sialic acid binding in human hemagglutinin (A/Aichi/68) depicted as ball and sticks (Table 1). Sialic acid is depicted as a black ball and stick model. Additional amino acids that occur in p37 and not in human hemagglutinin (A/Aichi/68) are depicted in green. Note the potential for steric clusters between Y202 of p37 and the binding of sialic acid.

functional role in receptor binding. However, it should be noted that p37 has a single amino acid (tyrosine) inserted at position 202 not found in either the avian or human form of hemagglutinin A (Fig. 4C). This tyrosine insertion is directly on the opening of the putative sialic acid binding site and may be there as a selective gate for receptor recognition or itself occupies the binding site, thus blocking sialic acid binding.

Neuraminidase treatment of prostate carcinoma cells before the addition of p37 decreased the binding of p37, whereas the addition of free sialic acid, or fetuin, a glycoprotein rich in sialic acid, enhanced binding of p37 to the cells (Table 2). Although the results indicate that 2,3-linked sialic acid may be important for p37 binding, they do not rule out a role for 2,6-linked sialic acid because binding was not completely abolished. The fact that sialic acid and fetuin enhanced, rather than reduced, sialic acid binding is consistent with a model wherein p37 binds sialic acid first, perhaps, to ''dock'' onto the cell, and then undergoes a conformational change wherein another domain of p37 binds a specific receptor. This model remains to be tested.

Taken together with the earlier evidence that autoimmune reaction to p37 correlates with tumor regression (15), these data further support the idea that p37-based therapeutics might be effective in cancer intervention. For example, whereas genetically engineered p37 might be used as an immunotheraputic agent to elicit a specific immune response in cancer patients, it might also increase the

Table 1. Conservation of residues in the sialic acid binding site of hemagglutinin A from avian and human A/Aichi/68 influenza virus compared with p37

Residue	p37	INF	HGG
Serine	204	133	136
Phenylalanine	214	143	147
Tryptophan	220	149	153
Histidine	250	179	183
Leucine	261	190	193

NOTE: The numbers given are the conserved amino acid positions for the structurally equivalent residues, for the model of p37 and sialic acid binding site of hemagglutinin A from avian (INF) and human A/Aichi/68 (HGG) influenza virus, respectively. The numbers are based on the sequence alignment shown in Fig. 3.

Table 2. The effect of neuraminidase treatment on the binding of p37 to PC-3 prostate carcinoma cells

Addition	% Binding
No addition	100 ± 4
α2,3 Neuraminidase	49 ± 11
α2-3,6,8 Neuraminidase	49 ± 15
Sialic acid	127 ± 8
Fetuin	194 ± 15

NOTE: PC-3 cells were treated with neuraminidase from either *A. ureafaciens* (removes terminal α2-3,6,8-linked sialic acid residues) or *M. decora* (removes only terminal α2,3-linked sialic acid residues), for 4 hours followed by 50 μg/mL p37. For the conditions with sialic acid (2.5 mmol/L) or fetuin (100 μg/mL), the compounds were mixed with p37 before addition to the cells. The two-antibody sandwich ELISA assay was employed for the detection of bound p37. Values are averages of triplicate results and SDs are reported.

DOI:10.1158/1535-7163.MCT-05-0040

metastatic activity of tumors present in the patient. Therefore, attempts at defining the specific regions of the p37 molecule responsible for the immunogenicity, as opposed to invasiveness enhancement, would be highly useful. Alternatively, the knowledge that p37 alone causes the observed enhancement of invasive potential suggests that a rational design of molecules that interfere with the interaction of p37 and tumor cell surface might diminish the invasive potential of p37 and possibly provide an important prevention for some cases of metastatic tumor progression.

References

1. Relman DA. The search for unrecognized pathogens. Science 1999; 284:1308 – 10.

2. Ley C, Parsonnet J. *Helicobacter pylori* infection and gastric cancer. Gastroenterology 2001;20:324 – 5.

3. Blaser MJ, Parsonnet J. Parasitism by the ''slow'' bacterium *Helicobacter pylori* leads to altered gastric homeostasis and neoplasia. J Clin Invest 1994;94:4 – 8.

4. Lo SC. Mycoplasmas: molecular biology and pathogenesis. In: Maniloff J, McElheney RN, Finch LR, Baseman JB, editors. Am. Soc. Microbiol. Press, Washington, DC. 1992. p. 525 – 45.

5. Waites KB, Taylor-Robinson D. Mycoplasma and ureaplasma. In: Murray PR, Baron EJ, Pfaller MA, Tenover FC, Yolken RH, editors. Manual of clinical microbiology. Chap. 56, Am Soc Microbiol Press, Washington, DC.; 1999.

6. Paton GR, Jacobs JP, Perkins FT. Chromosome changes in human diploid-cell cultures infected with Mycoplasma. Nature 1965;207:43 – 5.

7. Fogh J, Fogh H. Chromosome changes in PPLO-infected FL human amnion cells. Proc Soc Exp Biol Med 1965;119:233 – 8.

8. Macpherson I, Russell W. Transformations in hamster cells mediated by mycoplasmas. Nature 1966;210:1343 – 5.

9. Lindsey JR, Baker HJ, Overcash RG, Cassel GH, Hunt CE. Murine chronic respiratory disease. Significance as a research complication and experimental production with Mycoplasma pulmonis. Am J Pathol 1971; 64:675 – 708.

10. Cimolai N. Do mycoplasmas cause human cancer? Can J Microbiol 2001;47:691 – 7.

11. Sasaki H, Igaki H, Ishizuka T, Kogoma Y, Sugimura T, Terada M. Presence of streptococcus DNA sequence in surgical specimens of gastric cancer. Jpn J Cancer Res 1995;86:791 – 4.

12. Chan PJ, Seaj AM, Kalugdan TH, King A. Prevalence of mycoplasmas conserved DNA in malignant ovarian cancer detected using sensitive PCR-ELISA DNA. Gynecol Oncol 1996;63:258 – 60.

13. Kidder M, Chan PJ, Seaj IM, Patton WC, King A. Assessment of archived paraffin-embedded cervical condyloma tissues for mycoplasmas-conserved DNA using sensitive PCR-ELISA. Gynecol Oncol 1998;71: 254 – 7.

14. Quirk JT, Kupinski JM, DiCioccio RA. Detection of Mycoplasmal ribosomal DNA sequences in ovarian tumors by nested PCR. Gynecol Oncol 2001;83:560 – 2.

15. Fareed GC, Mendiaz E, Sen A, Juillare GJF, Weisenburger TH, Totanes TJ. Novel antigenic markers of human tumor regression. Biol Response Mod 1988;7:11 – 23.

16. Dudler R, Schmidhauser C, Parish RW, Wettenhall REH, Schmidt T. A mycoplasma high-affinity transport system and the *in vitro* invasiveness of mouse sarcoma cells. EMBO J 1988;7:3971 – 4.

17. Fareed GC, Sen A, Nuys V, Ghosh-Dastider P, Jar-How L. United States patent 5242823. 1998 Sept 7.

18. Ilantzis C, Thomson DMP, Michaelidou A, Benchimol S, Stanners CP. Identification of a human cancer related organ-specific neoantigen. Microbiol Immunol 1993;37:119 – 28.

19. Gilson E, Alloing G, Schmidt T, Claverys J-P, Dudler R, Hofnung M. Evidence for a high affinity binding-protein dependent transport system in Gram-positive bacteria and in Mycoplasma. EMBO J 1988;7: 3971 – 4.

20. Hogg A, Switzer WP, Farrington DO. Mycoplasmal diseases of swine. Colorado State University Cooperative Extension Livestock series; 1992.

21. Kobisch M, Friis NF. Swine mycoplasmoses. Rev Sci Tech 1996; 15:1569 – 605.

22. Steinemann C, Fenner M, Binz H, Parish RW. Invasive behavior of mouse sarcoma cells is inhibited by blocking a 37,000-dalton plasma membrane glycoprotein with Fab fragments. Proc Natl Acad Sci U S A 1984;81:3747 – 50.

23. Steinmann C, Fenner M, Parish RW, Binz H. Studies of the invasiveness of the chemically induced mouse sarcoma FS9. I. Monoclonal antibodies to a 37,000 dalton membrane glycoprotein inhibit invasion of fibroblasts *in vitro*. Int J Cancer 1984;34:407 – 14.

24. Schmidhauser C, Dudler R, Schmidt T, Parish RW. A mycoplasmal protein influences tumour cell invasiveness and contact inhibition *in vitro*. J Cell Sci 1990;95:499 – 506.

25. Huang S, Li JY, Wu J, Meng L, Shou CC. Mycoplasma infections and different human carcinomas. World J Gastroenterol 2001;7:266 – 9.

26. Zhang J, Wang Y, Shou C, et al. Detection of *Mycoplasma hyorhinis* in gastric cancer using bio-chip technology. Zhonghua Yi Xue Za Zhi 2002;82:961 – 5.

27. Gignac SM, Brauer S, Hane B, Quentmeier H, Drexler HG. Elimination of mycoplasma from infected leukemia cell lines. Leukemia 1991;5:162 – 5.

28. Pizao PE, Lyaruu DM, Peters GJ, et al. Growth, morphology and chemosensitivity studies on postconfluent cells cultured in 'V'-bottomed microtiter plates. Br J Cancer 1992;66:660 – 5.

29. Hendrix MJ, Seftor EA, Seftor RE, Fidler IJ. A simple quantitative assay for studying the invasive potential of high and low human metastatic variants. Cancer Lett 1987;38:137 – 47.

30. Band C, Sager R. Distinctive traits of normal and tumor-derived human mammary epithelial cells expressed in a medium that supports long-term growth of both cell types. Proc Natl Acad Sci U S A 1989;86: 1249 – 53.

31. Schmid SL, Carter LL. ATP is required for receptor-mediated endocytosis in intact cells. J Cell Biol 1990;111:2307 – 18.

32. Madden TL, Tatusov RL, Zhang J. Applications of network BLAST server. Methods Enzymol 1996;266:131 – 41.

33. Sauter NK, Hanson JE, Glick GD, et al. Binding of influenza virus hemagglutinin to analogs of its cell-surface receptor, sialic acid: analysis by proton nuclear magnetic resonance spectroscopy and X-ray crystallography. Biochemistry 1992;31:9609 – 21.

34. Jones TA, Zou J-Y, Cowan SW, Kjeldgaard M. Improved methods for binding protein models in electron density maps and the location of errors in these models. Acta Crystallogr A 1991;47:110 – 9.

35. Brunger AT, Adams PD, Core GM, et al. Crystallography and NMR system: a new software suite for macromolecular structure determination. Acta Crystallogr D Biol Crystallogr 1998;54:905 – 21.

36. Esnouf RM. An extensively modified version of MolScript that includes greatly enhanced coloring capabilities. J Mol Graph Model 1997; 15:132 – 4,112 – 3.

37. Wiley DC, Skehel JJ. The structure and function of the hemagglutinin membrane glycoprotein of influenza virus. Annu Rev Biochem 1987;56: 365 – 94.

38. Jia Z, Hasnain S, Hirama T, et al. Crystal structures of recombinant rat cathepsin B and a cathepsin B-inhibitor complex. Implications for structure-based inhibitor design. J Biol Chem 1995;270:5527 – 33.

39. Eisen MB, Sabesan S, Skehel JJ, Wiley DC. Binding of the influenza A virus to cell-surface receptors: structures of five hemagglutinin-sialyloligosaccharide complexes determined by X-ray crystallography. Virology 1997;26:19 – 31.

40. Martin J, Wharton SA, Lin YP, et al. Studies of the binding properties of influenza hemagglutinin receptor-site. Virology 1998;241:101 – 11.

41. Garten W, Klenk HD. Understanding influenza virus pathogenicity. Trends Microbiol 1999;3:99 – 100.